COOLING OF HIGH INTENSITY ATOMIC
HYDROGEN BEAMS TO LIQUID HELIUM TEMPERATURES*

A. Hershcovitch, A. Kponou, and T.O. Niinikoski[+]

AGS Department, Brookhaven National Laboratory
Upton, NY 11973 USA

ABSTRACT

An atomic hydrogen source, designed to operate in the laminar flow range, has
been built at BNL. A unique feature of this source is a miniature gap between
a teflon tube which guides the beam and an accommodator which cools it.
Across this gap a stepfunction in temperature, with the teflon temperature
exceeding 100 K and the accommodator temperature as low as 3 K, was success-
fully maintained. This configuration collimates the beam enough to prevent
significant diffusive losses without subjecting it to the temperature range of
high recombination. A record H^o beam flux of 3.32 x 10^{18} H^o/sr-sec was
obtained at an accommodator temperature of 5.5 K.

1. Introduction

Sources of polarized atomic hydrogen beams which are based on mag-
netic separation employ various forms of beam cooling. The advantage of cool-
ing hydrogen atoms before their exposure to a magnetic field gradient for spin
selection has been recognized for quite some time [1]. The force on an atom
due to the interaction of its magnetic moment with the magnetic field
gradient, is such as to minimize its potential energy which changes by μB at
high magnetic fields. However, for an atom to pass through such a magnet, its
energy associated with perpendicular motion must be lower than μB. Con-
sequently, an acceptance solid angle $\Delta\Omega$ is roughly determined by

$$\Delta\Omega \simeq \mu B/kT \ .$$

It is obvious from the above equation that by lowering the temperature by an
order of magnitude, the polarized beam flux should increase by the same
factor. Furthermore, for some ionizers, the ionization efficiency increases
with density, and if beam cooling can be accomplished with only minimal loss
of flux, another factor of $T^{-1/2}$ can be gained in the overall intensity of a
charged nuclear spin polarized beam.
        At BNL, an apparatus to test the possibility of cooling high in-
tensity atomic beams has been constructed. In this device, an atomic hydrogen
beam is produced by a conventional dissociator similar to that of PONI 1 [2].
The beam is guided by a teflon section into an accommodator which is cooled
by a cryostat to liquid helium temperatures. Cooling is achieved by colli-
sions with the cold accommodator surface. This apparatus is very similar to
other devices [3,4] in which low intensity beams have been successfully cooled
to the 5-8 K range. Walraven and Silvera's source [3] achieved an 8 K beam
with 2.4 x 10^{16} atoms/sec. Crampton [4] obtained 4.5 x 10^{13} polarized atoms/
sec at an accommodator temperature of 5.35 K. Our objective is to cool to
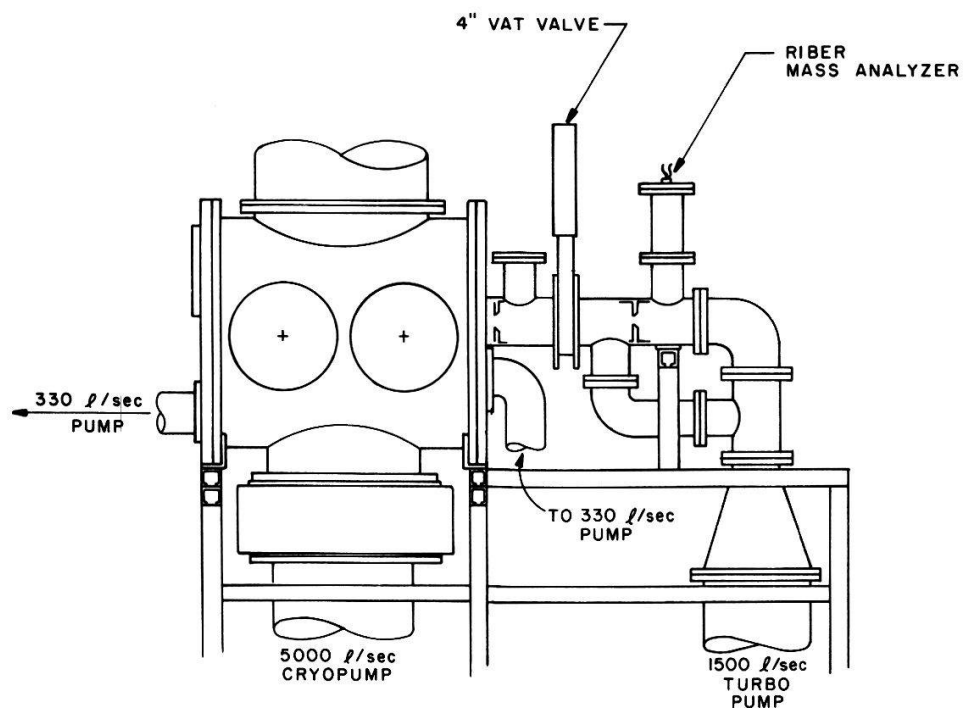that temperature range a beam of more than 10^{19} atoms/sec. Since most dis-

Figure 1.   Diagram of the experimental arrangement.   The cryostat is mounted
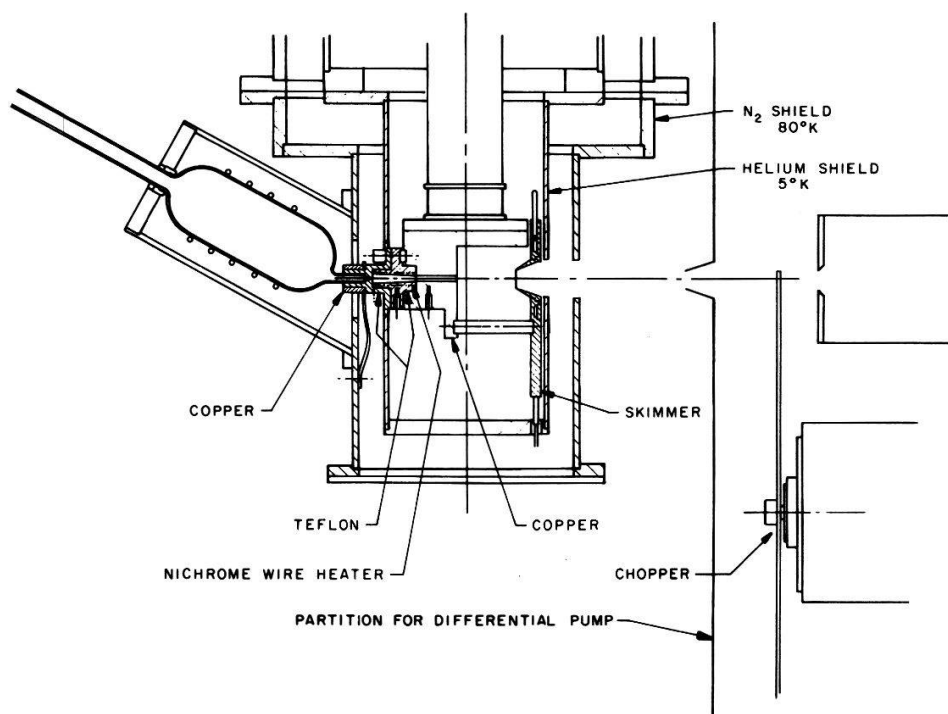on the top flange of the vacuum chamber.

Figure 2.   Details of the cold atomic source.

sociators operate in the same range of parameters, another way of comparing beam intensities is the size of the dissociator orifice. In Walraven's source the orifice area was 0.1 mm^2. In our first attempt we started with 0.8 mm^2 and we eventually reached over 9 mm^2. Our highest flux to date of 3.32 x 10^{18} H°/sr-sec is close to our objective of 10^{19} atoms/sec.

2. Experimental Apparatus

Figure 1 is a layout of the experimental arrangement. The main vacuum chamber is pumped by a 5000 ℓ/sec cryopump. A 300 ℓ/sec, (on the left), turbomolecular pump is used as a roughing pump while the other 300 ℓ/sec pump is used to differentially pump the chopper motor. Figure 2 shows details of what is housed in the vacuum chamber. Atoms are produced in a dissociator whose coil and enclosure form a resonant cavity. The dissociator nozzle has been cooled to liquid nitrogen temperature either by a strap tied to the 80 K shield, or by a cooling block whose temperature can be lowered via liquid nitrogen flow or elevated with a heater. The atoms are then guided by a short teflon tube into the accommodator. Since the teflon is between the 80 K nozzle and the liquid helium temperature accomodator, it is subjected to a temperature range of 10 K to 70 K. This is a bad temperature range since all materials have high recombination ratios at these temperatures and the temperature is not low enough for a frozen H$_2$ coating to be formed. At a low beam flux, the effect of the "bad" temperature range can be minimized by either restricting (3) this range to a small region in the teflon section where very few wall collisions occur, or by leaving a "large" gap (4) (cm) between the source orifice and the accommodator. Since the accommodator diameter is larger than that of the orifice, only a small part of the atomic beam is lost. For a high beam flux, where the flow is viscous, neither solution is acceptable due to the high collisionality of the gas and the large source orifice. The high collisionality makes even a 1 mm region of "bad" temperature unacceptable and the size of the source orifice combined with the high collisionality requires a very large accommodator diameter which is impractical. Our approach is to have a 0.3 mm gap between the teflon section and the accommodator which is enough to isolate them thermally. The teflon temperature is maintained above 80 K by means of a heater. In this way the beam is not subjected to a temperature range with high recombination probability and it is collimated enough to prevent significant diffusive losses.

After crossing the 0.3 mm gap, the atoms enter a 2 cm long accommodator with a diameter of 3 mm, whose temperature can be varied from 3 K to 300 K. A skimmer cooled down to 2.5 K is located 3 cm from the accommodator exit. A Riber residual gas analyzer (RGA), which is located 68.58 cm from the accommodator exit and is differentially pumped by a 1500 ℓ/sec turbomolecular pump, detects the atomic beam. In addition, there are collimators for further differential pumping between the accommodator and the detector. A chopper located 55 cm upstream from the RGA can be inserted into the beam path for time-of-flight measurements.

A conventional time-of-flight (TOF) set-up is used to measure beam velocity (5). Schematic diagrams of the apparatus and of the timing logic are shown in Figure 3. A dynamically balanced aluminum disk, 10 inches in diameter, with two diametrical slits 0.05 in wide chops the beam at √80 Hz. A smaller disk and photodiode/detector unit provide the reference signal. Beam geometry is defined by collimating apertures on either side of the chopper. Since the beam is pulsed, synchronization with the signal averager is essential. This is achieved with an interval counter which triggers the system after a preset number of reference pulses. Only one TOF spectrum is recorded
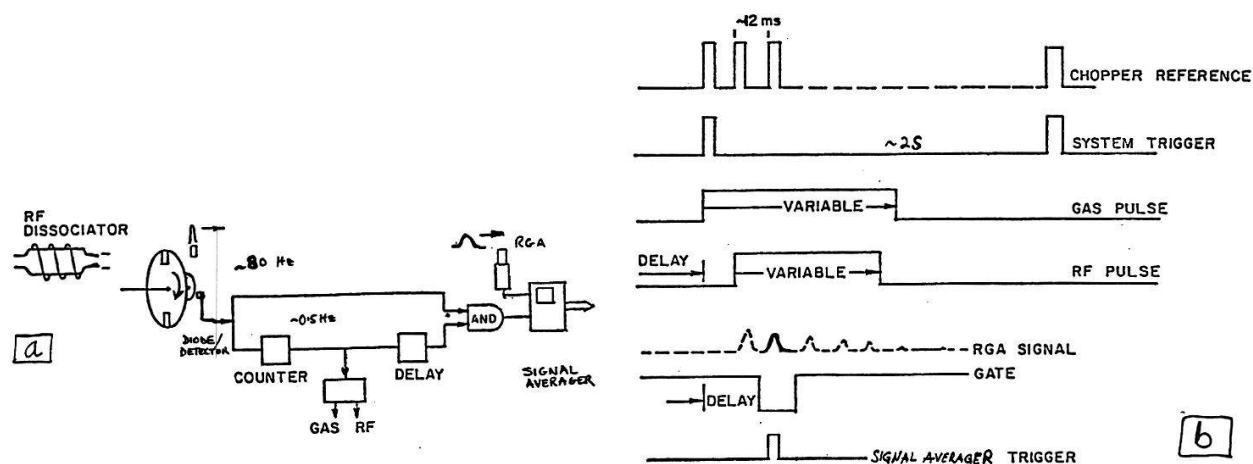
Figure 3. (a) Schematic of TOF apparatus.
           (b) Timing logic of the experiment.

for each beam pulse. Spectrum averaging, to improve the signal-to-noise ratio
is done under computer control (Apple IIe). The averaged spectra are analyzed
using Kubischta's (5) method, to obtain the velocity distributions.

3. Gas Dynamics in Nozzle and Accommodator

The properties of a molecular beam depend to a large extent on the
stagnation density, temperature and pressure of the gas before beam formation.
High-power RF discharge atom sources operate best at pressures around 3 Torr
at 300 K, which corresponds to an atomic density of about 10^{17} cm^{-3} and mean
free path of ground-state atoms around $\lambda = 60$ µm. The Knudsen number in
a channel of diameter d = 3 mm is then

$$K_n = \frac{\lambda}{d} \simeq 0.02$$

which means that the gas dynamics resembles slip flow of bulk gas rather than
free molecular flow. In calculating the flow characteristics in this regime,
we need to estimate the mass-flow rate, which has the upper limit given by the
isentropic discharge rate (choked flow)

$$\dot{m}^* = \psi^* \frac{PA_t}{a_o} \simeq 130 \ \mu g \ s^{-1} \tag{1}$$

in a throat of area A_t corresponding to an effective diameter of 3 mm. Here
$\psi^* = \gamma \left(2/(\gamma+1)\right)^{(\gamma+1)/2(\gamma-1)} = 0.94$, $\gamma = 1.67$ is the specific heat ratio for a
monatomic gas, $a_o = (\gamma RT)^{1/2}$ is the acoustic speed in stagnating gas, and P is
the stagnation pressure. We note that cooling of the gas in the discharge ori-
fice, while keeping the stagnation pressure constant, would increase the mass
rate proportional to $T^{-1/2}$, assuming that the cooling will not result in the re-
combination of the atoms on the walls providing heat exchange. On the other
hand, if the density of the stagnating gas near the orifice is limited due to
recombination processes, then the flow of atoms out of the orifice decreases
with decreasing temperature proportional to $T^{+1/2}$.

In the accommodator channel of diameter D = 3 mm the Reynolds number
for the flow corresponding to Eq. (1) is

$$N_{Re} = \frac{DG}{\mu} = 10.65 \tag{2}$$

taking the viscosity μ at an average temperature of 30 K. N_{Re} varies as $T^{-1/2}$, which assures that the flow is always laminar.

In the following we shall discuss the gas dynamics in our apparatus which is shown schematically in Figure 4. The gas properties in the dissociator and at the accommodator entry and exit points are labeled by subscripts 0, 1 and 2, respectively, as shown in Figure 4. Furthermore, the gas properties on the freezing surface are labeled by the subscript f. The stagnation temperature, pressure and density at each point x is expressed as T_x, P_x and n_{0x}; the local (dynamic) properties are expressed as t_x, p_x and n_x. The local Mach number is written $M_x = V_x/a_x$, where V_x is the local gas velocity and a_x the local acoustic speed at the point x.

In an attempt to understand the gas dynamics in our channel of constant area, let us consider steady one-dimensional flow with friction, and assume first that the flow is adiabatic (no heat exchange with walls). By requiring that the enthalpy and mass are conserved, the gas properties will be given by (7)

$$\frac{dp}{v} + G\left(\frac{dv}{v} + \frac{1}{2}\frac{4f\,dx}{D}\right) = 0 \tag{3}$$

where p and v are the dynamic pressure and specific volume in the gas flow, and f is the friction factor given by

$$4f = \frac{64}{N_{Re}} \tag{4}$$

for laminar flow. The local dynamic density $n = \rho/m_H$ and the stagnation pressure P are reduced by the frictional losses in a way which depends on the flow velocity V or local Mach number $M = V/a$:

$$\frac{dn}{n} = -\frac{\gamma M^2}{2(1-M^2)}\frac{4f\,dx}{D}\ ; \tag{5}$$

$$\frac{dP}{P} = -\frac{\gamma M^2}{2(1-M^2)}\frac{4f\,dx}{D}\ . \tag{6}$$

We note that in a long channel M cannot reach a value near 1 because such a drop in the density and stagnation pressure would happen that the upstream conditions would have to be changed, if $4f = 64/N_{Re} \simeq 6.4$. The flow is therefore choked by the frictional forces in the channel rather than by the sonic velocity in a throat; considering isothermal flow the maximum speed is then

$$V_{max} = \frac{a}{\sqrt{\gamma}} \tag{7}$$

and the inlet mass flow rate can be calculated by solving the inlet Mach number M_0 from the equation

$$\frac{4fL}{D} = \frac{1-\gamma M_0^2}{\gamma M_0^2} + \ln\left(\gamma M_0^2\right)\ , \tag{8}$$

where L is the length of the isothermal section.

The pressure p_1 at the choking limit is

$$p_1 = p_0 M_0 \sqrt{\gamma} \tag{9}$$

which allows us to calculate the outlet state of the gas in the isothermal frictional choke. We remind here that p_0 and M_0 are the gas properties downstream of the dissociator throat, in which the flow is supposed to be isentropic.

In our case there may be a large temperature gradient in the accommodator channel between the throat and the accomodator; a much more complicated equation must then be solved to find the rate of a steady flow. We are satisfied here with the approximate solution of Eq. (8).

$$M_0 \simeq \frac{D}{4fL\gamma} \cdot \tag{10}$$

By inserting the friction factor $4f$ and N_{Re} from Eqs. (4) and (2) into Eq. (10) and expressing the inlet Mach number M_0 as $M_0 = \dot{m}(\rho A a_1)^{-1}$, we may solve the flow rate

$$\frac{\dot{m}}{\rho} = \frac{p_0}{2Z_0\mu} , \tag{11}$$

where

$$Z_o = \frac{128L}{\pi D^4} \tag{12}$$

is the flow impedance of the isothermal section of the circular pipe which chokes the flow. The pressure in the accommodator now becomes

$$p_1 \simeq \frac{p_0^2}{2Z_o\mu A a_1} \tag{13}$$

which will define the state of the gas before the final expansion to the beam vacuum, once the temperature is established.

As an example, our configuration resembles a tube of 0.3 cm diameter and 1 cm length at 300 K temperature; for $p_0 = 3$ torr this gives $M_0 = 0.212$ and $p_1 = 0.823$ torr. At this low Mach number the flow is almost incompressible, and the subsequent pressure drop in the accommodator may be estimated by taking the worst-case linear temperature distribution from inlet temperature $T_1 = T_0$ to the outlet temperature $T_2 \simeq T_a$:

$$\Delta p_a = \frac{2}{5} Z \mu_0 \dot{v}_1 \frac{T_1^{5/2} - T_2^{5/2}}{T_1^{3/2}(T_1 - T_2)} \simeq \frac{2}{5} Z_a \mu_0 \dot{v}_1 .$$

By approximating the inlet volume flow $\dot{v}_1$ by the volume flow out of the discharge $\dot{v}_0$ given by Eq. (11), we get

$$\Delta p_a = \frac{2}{10} \frac{Z_a}{Z_o} p_1 = \frac{2}{10} \frac{L_a}{L} p_1 \cdot \tag{14}$$

We may conclude that by assuming the pressure in the accommodator constant and equal to the limiting pressure of frictionally choked flow given by Eq. (13), the percentage overestimate is less than 20% of the impedance or length ratio of the accommodator section with a large thermal gradient, and the isothermal choking section. We shall assume here that the pressure in the accommodator is constant and equal to the p_1 of Eq. (9). We note also that at $M \simeq 0.2$ the gas dynamic effects may be practically neglected, and the fluid may be regarded as incompressible, which greatly simplifies the calculation of heat transfer using the effectiveness-N_{tu} approach.

The effectiveness ε of a heat transfer process is defined as the amount of heat transferred divided by the maximum possible heat transfer. For a perfect gas flowing through our isothermal accommodator at temperature T_a this becomes

$$\varepsilon = \frac{T_1 - T_2}{T_1 - T_a} , \tag{15}$$

where T_1 and T_2 are the inlet and outlet temperatures of the flowing gas. The effectiveness can be approximated by calculating the average film heat transfer coefficient $\bar{h}_c$ for the laminar bulk flow:

$$\bar{h}_c = \langle N_{Nu} \kappa/D \rangle , \tag{16}$$

where the Nusselt number is

$$N_{Nu} = 3.65 + \frac{0.0668(D/L)N_{Re}N_{Pr}}{1 + 0.04 \left[(D/L)N_{Re}N_{Pr}\right]^{2/3}} \tag{17}$$

and the heat conductivity is

$$\kappa = \frac{5}{4} \rho\lambda\langle v \rangle c_v \simeq 3.9 \left(\frac{T}{300 \text{ K}}\right)^{1/2} \frac{mW}{cmK} . \tag{18}$$

Because of the very small Reynolds number $N_{Re} \simeq 10$, even at the isentropically choked maximum flow of Eq. (1), the Nusselt number is practically constant $N_{Nu} = 3.69$, and $\bar{h}_c$ may be taken to correspond to a value of $h_c(T)$ at $T = 30$ K, for example. This gives

$$\varepsilon = 1 - e^{-N_{tu}} , \tag{19}$$

where

$$N_{tu} \simeq \frac{\bar{h}_c A_h}{\stackrel{\bullet}{n} c_v} , \tag{20}$$

A_L is the total heat transfer surface area $A_h = \pi D L_a$ in a circular accommodator, and $\stackrel{\bullet}{n} c_v$ is the flow heat capacity. With the most adverse condition of maximum flow in our geometry we get $N_{tu} \simeq 10.4$, which gives

$$T_2 - T_a = (T_1 - T_a)(1 - \varepsilon) = (T_1 - T_a)e^{-N_{tu}}$$
$$= 3.10^{-5}(T_1 - T_a). \tag{21}$$

It is clear that in our case the actual temperature distribution is not as steep as Eq. (19) might suggest, because the axial conduction in the flowing gas cannot be neglected in our short (L_a = 3 cm) accommodator. However, the result (21) is a good approximation and allows us to conclude that for T_1 = 300 K (for example), the outlet temperature T_2 is no more than 10-100 mK above the accommodator wall temperature T_a.

The cooling of the flowing gas in the accommodator will increase the Mach number and eventually the flow becomes choked at M = 1 if the frictional forces are neglected (which is not our case). However, this cooling has the effect of increasing the dynamic density of the gas by

$$\frac{dn}{n} = -\frac{(1 + \frac{\gamma - 1}{2} M^2)}{1 - M^2} \frac{dT}{T} \tag{22}$$

which has the beneficial effect of compensating some of the density loss due to frictional forces, given by Eq. (5). If the flow did become choked by cooling, the limiting density is given by

$$n^* = n \frac{(\gamma + 1)M^2}{1 + \gamma M^2}, \tag{23}$$

where n and M refer to the point of entry to the cooling channel of constant area. A subsequent diffuser with additional cooling would then enable us to substantially increase n before entering into the beam-forming orifice; however, in our present case the frictional forces prevent us from doing this, and three-body recombination would probably prevent any gain from this.

To summarize, we have learned that an accommodator can be designed which satisfies the criteria of good heat transfer and geometry favourable for keeping recombination losses to a minimum. The flow in such an accommodator, however, is likely to be dominated by frictional forces rather than other gas dynamic phenomena in steady state.

The transient behavior of flow will be qualitatively discussed below and compared to the experimental results.

4. Beam Formation

When the atomic beam exits the nozzle, as shown in Figure 4 it expands isentropically into the vacuum and cools. The vacuum space may be approximated as a semi-infinite continuum. The expansion continues until the mean free path grows so long that the gas can be thought to undergo collisionless molecular flow. At that point the supersonic velocity distribution freezes in and no further cooling due to expansion will occur. The local density of the expanding gas is given by

$$n = n_{02} \left(1 + \frac{\gamma - 1}{2} M^2\right)^{-\frac{1}{\gamma - 1}} \tag{24}$$

and the mean free path λ_f at the freezing point may be taken equal to

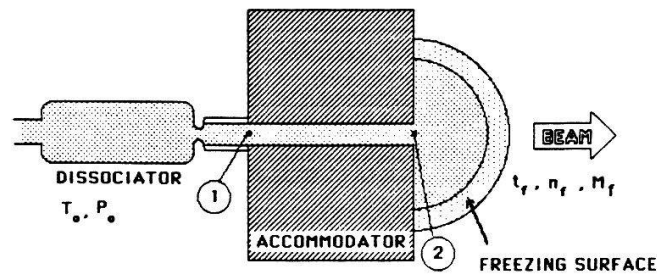$$\lambda_f = \eta \cdot r_f = \frac{1}{\sqrt{2}\pi d^2 n_f} \tag{25}$$

Figure 4

where d is the atomic diameter, r_f is the radius of the half-spherical freez-
ing surface A_f, and η is a numeric coefficient, which we shall assume equal to
unity here. The Mach number M_f corresponding to the surface A_f can be solved
from the continuity equation

$$\frac{\dot{m}}{A_f P_2} \left(\frac{RT_2}{\gamma}\right)^{1/2} = M_f \left(1 + \frac{\gamma - 1}{2} M_f^2\right)^{-\frac{\gamma + 1}{2(\gamma - 1)}}, \tag{26}$$

where $A_f = 2\pi r_f^2$, P_2 is the stagnation pressure at the end of the accommoda-
tor, and $\dot{m} = \rho_2 A V_2$. By expressing the gas property ratios in terms of the
Mach number $M_2 = V_2/a_2 = V_2/\sqrt{\gamma R t_2} = V_2/\sqrt{\gamma R T_a}$, we get

$$\left(\frac{\pi}{2} \eta d^2 n_2\right)^2 M_2 F(M_2) = M_f F(M_f), \tag{27}$$

where

$$F(M) = \left(1 + \frac{\gamma - 1}{2} M^2\right)^{\frac{3 - \gamma}{2(\gamma - 1)}}. \tag{28}$$

The density on the freezing surface n_f is

$$n_f = n_2 \left(\frac{1 + \frac{\gamma - 1}{2} M_2^2}{1 + \frac{\gamma - 1}{2} M_f^2}\right)^{\frac{1}{\gamma - 1}}. \tag{29}$$

These allow us to calculate the beam flux, density and velocity distribution
at any point, once the n_2 and M_2 are known on the basis of gas dynamics and
recombination kinematics in the accommodator.

Let us first suppose that there is no recombination in the accommoda-
tor, and that the flow becomes frictionally choked at the nearly isothermal
section in the end. This gives $M_2 = \gamma^{-1/2}$ and $n_2 = (T_0/t_2)n_0 = (T_0/T_a) n_0$.
It is clear that for $T_0/T_a \simeq 10-50$ the volume recombination (three-body col-
lisional processes) will start limiting the density n_2, if the discharge op-
erates at $n_0 = 10^{17}$ cm^{-3}.

Assuming $\eta = 1$ we now get from Eqs. (25) and (29)

$$r_f = \frac{1}{\sqrt{2}\pi d^2 n_2} \cdot \left(\frac{1 + \frac{\gamma - 1}{2} M_f^2}{1 + \frac{\gamma - 1}{2} M_2^2} \right)^{\frac{1}{\gamma - 1}} \tag{30}$$

and the density beyond r_f at any distance R from the end of the accommodator is given by

$$n(R) = \left(\frac{r_f}{R}\right)^2 n_f = \frac{1}{2\pi^2 d^4 n_2 R^2} \left(\frac{1 + \frac{\gamma - 1}{2} M_f^2}{1 + \frac{\gamma - 1}{2} M_2^2} \right)^{\frac{1}{\gamma - 1}} \tag{31}$$

and velocity by

$$V_f = M_f \sqrt{\gamma R t_f} = \sqrt{\gamma R T_a} \; M_f \left(\frac{1 + \frac{\gamma - 1}{2} M_2^2}{1 + \frac{\gamma - 1}{2} M_f^2} \right)^{\frac{1}{2}}, \tag{32}$$

where $M_2 = \gamma^{-1/2}$, T_a is the accommodator surface temperature, and M_f is a function of n_2 obtained by numerically solving the Eq. (27). Furthermore, the velocity distribution is given by

$$n(V) = C \cdot V^2 e^{-\frac{(V - V_f)^2}{2 R t_f}}, \tag{33}$$

where C is the normalization constant and

$$t_f = T_a \frac{1 + \frac{\gamma - 1}{2} M_2^2}{1 + \frac{\gamma - 1}{2} M_f^2}. \tag{34}$$

We conclude that once n_2 and T_a are determined, all measurable beam properties are fixed by Eqs. (31)-(34). Unfortunately there is no way to directly measure n_2; instead we may compare the consistency of T_a, V_f, M_f and n(R). Assuming that $n_2 = 0.5 \times 10^{17}$ cm^{-3} which is rather close to the limit of three-body recombination, we get the results given in Table 1. The record value of n(R) was obtained by exceeding the voltage rating of the dissociator power supply for short periods. With a modified dissociator values exceeding 1.3×10^{10} cm^{-3} were observed, however, the operation was unreproducible. The accommodator temperature in these cases was 5.5 K.

5. Experimental Results

The atomic hydrogen density is determined from the RGA signal. The numerical value is based on the calibration of this RGA against a calibrated ion gauge (done by the AGS vacuum group) for molecular hydrogen and based on the relative sensitivity of this RGA to molecular and atomic hydrogen. During the course of this study the dissociator aperture was increased in diameter from 1.27 mm to 2 mm to 3 mm, and so did the atomic hydrogen output. A record H^o density and flux was obtained at 5.5 K during operation in which the vol-

Table I. Comparison of the experimental results at T_a = 26.1 K and 6 K with the theoretical prediction assuming n_a = 0.5 x 10^{17} cm^{-3}.

Temp. Parameter	T_a = 26.1 K		T_a = 6 K	
	Exp	Th	Exp	Th
V_f (m/s)	714 ± 318	1019	590 ± 87	524
M_f	1.9	5.85	4.2	5.85
$n(R)$ (cm^{-3})	9 x 10^9	5.2 x 10^{10}	7 x 10^9	5.2 x 10^{10}
(record $n(R)$)			(10^{10})	

tage of the dissociator power supply was increased above the recommended limit.

Our record flux at 5.5 K stands at

$$3.32 \times 10^{18} \ H^\circ/sr\text{-}sec \ .$$

In normal operation the flux at this temperature (5-6 K) is about 2 x 10^{18} H$^\circ$/sr-sec. At temperatures of about 27 K the flux is about 5 x 10^{18} H$^\circ$/sr-sec.

The velocity distribution as measured by TOF is indicative of supersonic flow as Figure 5 shows. The flux is calculated from the product of the density and velocity divided by the solid angle which the RGA samples.

Keeping all parameters constant and scanning the accommodator temperature (Fig. 6) reveals some interesting features: at temperatures below 6 K the behavior is similar to that observed by Crampton et al. [4]. Above 6 K the H$^\circ$ signal drops by a factor of 2 at about 10 K. As the accommodator temperature is increased above 20 K, the H$^\circ$ signal increases until the accommodator temperature approaches 30 K at which point the H$^\circ$ signal drops sharply, and does not reach the previous values until T_a is reduced below 20 K.

A behavior similar to that of Figure 6 was observed even with dissociator apertures of 1.27 mm and 2 mm. However, at smaller orifice diameters, the lower temperature peak occurred at about 8-9 K and the signal did not drop quite as sharply at T_a > 30 K. Nevertheless, for 5 K < T_a < 30 K the H$^\circ$ signal varied by a factor of 2 only. This may indicate that recombinations and other loss processes are volume rather than surface dominated. Also, changes in the nozzle temperature had little effect.

Finally, the instantaneous H$_2$ gas flow in the piezoelectric valve was measured to be about 120 µg/sec, which is very close to the isentropic limit in a ϕ 3 mm dissociator orifice given by Eq. (1). The agreement is accidental, because the large volume of the dissociator bottle averages the gas flow over a time much longer than the 10 msec gate time of the valve; this was verified by observing the H$_2$ signals without RF discharge. With RF-discharge (triggered at optimized time delay) the atomic hydrogen signal at the RGA shows the following transient behavior: rise time typically 0.2 - 0.5 msec, to reach a sharp peak after which the signal droops almost exponentially to reach 0.5 to 0.2 times the peak value, during the 10 msec period corresponding to the length of the RF pulse. We tentatively explain the signal droop by the filling of the volume between the accommodator and the skimmer with H gas, which is only cryopumped on the 2.5 K skimmer after conversion to H$_2$ on the H$_2$-coated cold walls. This cold background gas gradually changes the initial isentropic

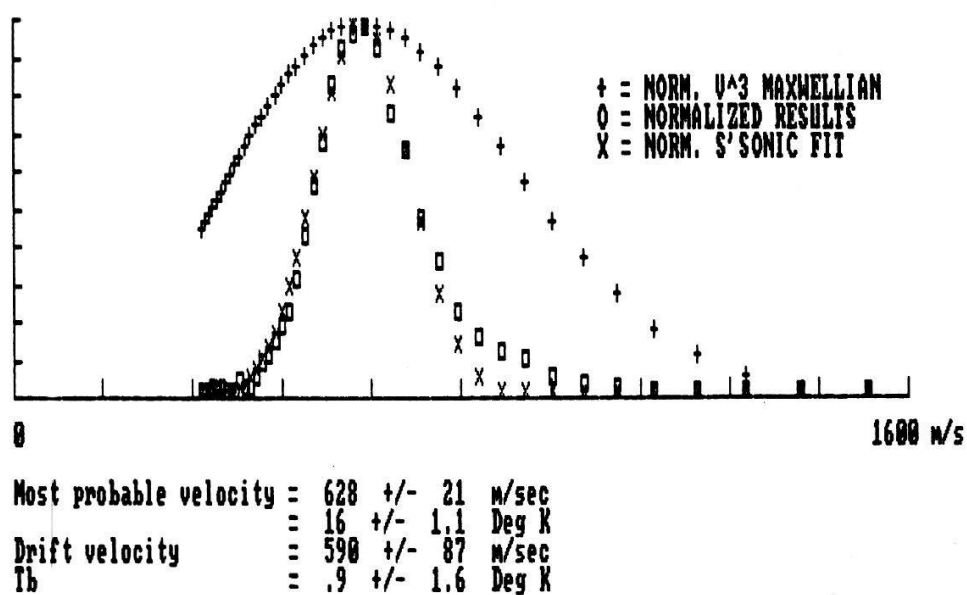| Most probable velocity | = 628 +/- 21 m/sec |
	= 16 +/- 1.1 Deg K
Drift velocity	= 590 +/- 87 m/sec
Tb	= .9 +/- 1.6 Deg K

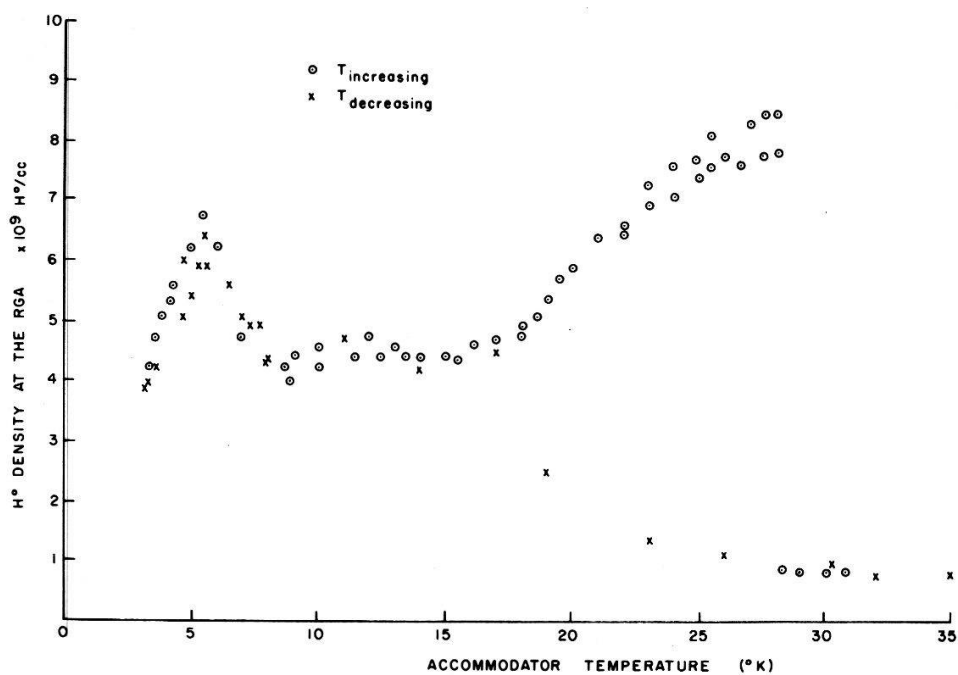Figure 5. Velocity distribution of H°. Rectangular boxes designate actual
data points.

Figure 6. H° density versus accommodator temperature.

expansion to vacuum, into lossy flow and molecular effusion at the skimmer orifice. This is observed also as a slowly decaying tail in the H signal after the RF-pulse. Furthermore, the velocity distributions in the beginning, center and end of the RF gate show a time evolution indicative of expansion into background gas of gradually increasing pressure.

If the dissociation were 100% and if there were no losses, the H^o flux would have been 7.2×10^{19} H^o/sec or 1.14×10^{19} $H^o/sr-sec$, neglecting gas flow features and the possible beam spread non-uniformity. Our peak H^o signal at 5.5 K is a factor of 3.45 lower while routine operation at 27 K shows an H^o signal which is only 2.29 lower. Thus, if the dissociation is closer to 50%, then one concludes that at 27 K the H^o output is close to what we would expect and that wall recombination is not severe.

We would like to thank Dr. Th. Sluyters for initiating this project and B. Devito, R. Meier, W. Hansel and W. Tramm for excellent engineering and technical support. One of us (A.H.) would like to thank Dr. J. Walraven for useful discussions.

6. References

(1) Described in a number of review papers, e.g., W. Haeberli in the Proc. of the Third International Symposium on the Production and Neutralization of Negative Ions and Beams, K. Prelec, Editor, Brookhaven National Laboratory, 685 (1983). AIP Conference Proceedings No. 111.

(2) See paper by J. Alessi, et al., in these Proceedings.

(3) J.T.M. Walraven and I.F. Silvera, Rev. Sci. Instr. 53, 1167 (1982).

(4) S.B. Crampton, K.M. Jones, G. Nunes and S.P. Souza, Proc. the Precise Time and Time Interval Planning Meeting, Goddard Space Flight Center, November 27-29, 1984.

(5) Wen S. Young, R.S.I. 44 (1973) 715.

(6) W. Kubischta, CERN Report PS/DL/Note 77-5 (1977)

(7) M.J. Zucrow and J.D. Hoffman, Gas Dynamics, Wiley, N.Y. (1976).

Secretary's report, Session (C), T.B. Clegg:

W. Kubischta : a) Do you do anything special to your accommodator?
Answer   There is no special surface treatment, except for the time it takes to build up a surface layer of molecular hydrogen.
                  b) How clean must the gas be?
Answer   We use 99.99% pure hydrogen.
                  c) Have you ever tried to run d.c.?
Answer   We cannot. The cryopump capacity does not allow this.

D. Kleppner : Is it not peculiar that the intensity drops so quickly, after the discharge is turned off?
Answer   This is not understood.